



Optimal fuzzy logic control for MDOF structural systems using evolutionary algorithms

Sk. Faruque Ali, Ananth Ramaswamy*

Department of Civil Engineering, IISc, Bangalore 560012, India

ARTICLE INFO

Article history:

Received 10 August 2007

Received in revised form

27 August 2008

Accepted 13 September 2008

Available online 13 November 2008

Keywords:

Structural control

Fuzzy logic control

Genetic algorithms

Particle swarm optimization

Optimal fuzzy rule base

ABSTRACT

The paper presents an optimal fuzzy logic control algorithm for vibration mitigation of buildings using magneto-rheological (MR) dampers. MR dampers are semi-active devices and are monitored using external voltage supply. The voltage monitoring of MR damper is accomplished using evolutionary fuzzy system, where the fuzzy system is optimized using evolutionary algorithms (EAs). A micro-genetic algorithm (μ -GA) and a particle swarm optimization (PSO) are used to optimize the FLC parameters. Two cases of optimal FLCs are shown. One where FLC is optimized keeping the rule base predefined and in the other case, FLC rule base is also optimized along with other FLC parameters. The FLC rule base and membership function parameters are optimized using 10 variables. Fuzzy controllers with a predefined rule base and with an optimal rule base are applied to a single degree of freedom (SDOF) and a multi-degree of freedom (MDOF) system. Finally, the study evaluates the performance of the fuzzy controller optimized off-line, on a three storey building model under seismic excitations. The main advantage of using FLC to drive the MR damper voltage is that it provides a gradual and smooth change in voltage. Consequently, the present approach provides a better vibration control for structures under earthquake excitations.

© 2008 Elsevier Ltd. All rights reserved.

1. Introduction

Present day structures are built to be large, slender and flexible (e.g., long-span bridges, high-rise buildings, etc.) and are designed to serve more critical functions. However, large flexible structures subjected to natural disturbances such as wind gusts or earthquakes, experience large vibrations which may introduce damages in the structure. This may lead to moderate to large damage in structures and/or cause discomfort to the users. Specifically, in seismic dominant regions, earthquakes pose a serious threat to both the infrastructure and human lives. The protection of civil structures, including their material content and the human occupants, is without doubt a priority for structural designers worldwide. The extent of the protection may range from reliable operation and occupant comfort to human and structural survival under the action of these hazardous loads.

The use of external devices (control devices) to mitigate structural vibration during earthquakes as a means of hazard reduction has become popular over the last 10 years (Soong and Spencer, 2002). The design philosophy is to reduce the structural

responses to safe levels with limitations on both the control force applied (limited by the number and capacity of actuators and the required amount of energy to drive the system) and the number of measured signals (limited by number of sensors used). Depending on the level of energy required and the devices employed, a structural control system can be classified into passive, active, semi-active and hybrid systems (Ali and Ramaswamy, 2007). Among these systems, the semi-active control has recently received considerable attention, because it offers significant adaptability without a large power requirement. The magneto-rheological (MR) damper, which employs MR fluid to provide its controllable characteristics, is one of the newest additions to this family. Besides its low-power requirement, the MR damper is reliable, fail-safe against power cut, relatively inexpensive and amenable for full-scale structural control applications (Yang et al., 2002).

The nonlinear nature of MR dampers makes the design of a suitable control algorithm that can take advantages of the unique characteristics of these devices, an interesting and challenging task. MR dampers hysteretic behaviour are monitored using an external voltage supply, which makes damper supply voltage as a control variable. Numerous control algorithms for the control of the MR systems are proposed and reported. These include 'skyhook' damper control algorithm by Karnopp et al. (1974), proposed for a vehicle suspension system. This was followed by a

* Corresponding author. Tel.: +91 80 22932817; fax: +91 80 23600404.

E-mail addresses: skfali@civil.iisc.ernet.in (Sk.F. Ali), ananth@civil.iisc.ernet.in (A. Ramaswamy).

bang–bang controller (Feng and Shinozuka, 1990); direct Lyapunov based control algorithms (Leitmann, 1994); a modified homogeneous friction algorithm (Jansen and Dyke, 2000) and widely used clipped optimal strategy (Dyke et al., 1996).

These algorithms provide either zero or the maximum voltage value (without any intermediate levels of voltage supply) to the MR damper based on feedback from the structure. Thus these methods provide sub-optimal control force to the system. Moreover, swift changes in voltage supply lead to a sudden rise in the external control force which increases the system responses and may introduce local damages in the structure (Ali and Ramaswamy, 2008a). Therefore, there is a need for control algorithms that can change the MR damper voltage gradually and smoothly. This gradual change in MR damper supply voltage will enable a designer to cover all voltage values between zero and maximum voltage supply.

This paper presents an optimal fuzzy logic based approach to monitor the voltage supply to MR dampers. Some characteristics of FLC appealing to control engineers are their effectiveness and ease in handling structural nonlinearities, uncertainties and heuristic knowledge. Added to the niceties present in a fuzzy system, a fuzzy control applied to structural system can handle the hysteretic behaviour of the structure under earthquake (Dyke et al., 1996). Moreover, it provides an added robustness to the closed loop system when combined with MR dampers (Ali and Ramaswamy, 2006). Another advantage of the present FLC model used in conjunction with MR damper is that unlike in clipped optimal and Lyapunov control techniques, the change in voltage input to the MR damper is gradual and therefore it covers all voltage values in the range of zero and maximum damper voltages. This particular advantage not only permits the designer to use variable voltage value but also provides an inherent stability to the closed loop system.

Although fuzzy logic results in the creation of simple control algorithms, the tuning of the fuzzy controller is a more difficult and sophisticated procedure than that employed in conventional control algorithms (e.g., LQG, Lyapunov methods, etc.). Previous studies on optimal FLCs mainly focused on adaptively changing the fuzzy membership function (MF) parameters using genetic algorithm (GA), while predefining the rule base and retaining it unaltered (Ahlawat and Ramaswamy, 2004; Dounis et al., 2007; Ali and Ramaswamy, 2007). It will be shown in this study that a fixed rule base FLC (where rule base is eventually decided based on designer knowledge) is not as efficient as a variable rule base FLC in controlling the vibration of structures. Particularly when structures are subjected to seismic excitations, they vibrate in combination of different modes whose participation factors depend on the energy content of the excitation at a particular frequency (Chopra, 2005). This makes the manual design of an optimal rule base, a complex task.

In this paper, optimal FLC is constructed using micro-genetic algorithm (μ -GA) and particle swarm optimization (PSO). Both the μ -GA and PSO are stochastic search techniques but follow different methods to determine their next generation. PSO uses a simple algorithm and is easy to implement. Compared to GA, PSO takes less time for each function evaluation as it does not use many of the GA operators (like, mutation, crossover and selection operator). On the other hand, PSO is likely to stick to the optima it finds and stops exploring other regions (Kennedy and Eberhart, 1999). Micro-GA is similar to a simple GA but with a smaller initial population. It restarts its search space once an optima is found. Therefore, it has the ability to search a bigger space with reduced number of function evaluations. Both the techniques are used in this paper and compared. Relative merits and demerits are also highlighted.

Next section provides a brief description of the mathematical model of a MR damper used in this study. The implementation

details for both kind of FLCs using evolutionary algorithms (EAs) are discussed thereafter. Details of μ -GA, PSO and optimal FLC are given in the following section. Numerical simulations on a single degree of freedom (SDOF) and a multi-degree of freedom (MDOF) systems with both the forms of FLC for an impulsive force and support displacement, respectively, are then reported. Finally, the proposed FLC is applied to a three storey building vibration control problem under a set of earthquake records.

2. MR damper model

MR fluids belong to the class of controllable fluids. The essential characteristic of MR fluids is their ability to reversibly change from free-flowing, linear viscous Newtonian fluids to semi-solid Bingham fluids having a controllable yield strength when exposed to a magnetic field. This feature provides a simple, quiet and a rapid response interface between the electronic control and the mechanical system. MR fluid dampers are relatively inexpensive, compact, reliable, and stable. The device can provide controllable force just working on a battery power. Commercial MR dampers come with a Wonder Box[®] which is used to vary the magnetic flux across the MR damper. Wonder Box[®] takes external voltage as an input making the choice of voltage as an input variable to the MR damper, a viable one in preference to current. Because the semi-active device can only absorb vibratory energy from the structure by responding to its motion, it is considered to be stable (in a bounded-input, bounded-output sense) (Ikhouanea et al., 2005). Thus, semi-active devices are expected to offer effective performance over a variety of amplitude and frequency ranges. The first application of MR dampers to protect civil engineering structures has been conducted by Spencer and coworkers (Dyke et al., 1996).

2.1. MR damper model

Different models have been developed and reported in the literature to describe the behaviour of MR dampers (Spencer et al., 1997). For the present numerical study a simple Bouc–Wen hysteretic model (Spencer et al., 1997; Ali and Ramaswamy, 2008b) is considered. The equations governing the force produced by this model are given as

$$\begin{aligned} u(t) &= k_0 x(t) + c_0 \dot{x}(t) + \alpha z(t, x) \\ \dot{z} &= -\gamma |\dot{x}| z |z|^{n-1} - \beta \dot{x} |z|^n + A \dot{x} \end{aligned} \quad (1)$$

where x is the displacement at the damper location; z is the evolutionary variable and γ , β , n and A are parameters controlling the linearity in the unloading and the smoothness of the transition from the pre-yield to the post-yield region. k_0 , c_0 and α_0 are voltage dependent parameters. The functional dependence of the device parameters on the command voltage v_c is expressed as follows:

$$\begin{aligned} \alpha(v_c) &= \alpha_a + \alpha_b v_c \\ c_0(v_c) &= c_{0a} + c_{0b} v_c \\ k_0(v_c) &= k_{0a} + k_{0b} v_c \end{aligned} \quad (2)$$

where k_{0a} , k_{0b} , c_{0a} , c_{0b} , α_{0a} and α_{0b} are constant parameters whose numerical values are given in Table 1 and are taken from Ali and Ramaswamy (2008b). In addition, the resistance and inductance present in the MR damper circuit introduces dynamics in the system. This dynamics is accounted for by a first order filter on the voltage input, given by

$$\dot{v}_c = -\eta(v_c - v) \quad (3)$$

Table 1
MR damper parameter values

Parameter	Value
α_a	$1.9504 \times 10^5 \text{ N m}^{-1}$
c_{0a}	$8.666 \times 10^2 \text{ N s m}^{-1}$
k_{0a}	$7.5140 \times 10^2 \text{ N s m}^{-1}$
n	2
A	12.26
η	190 s^{-1}
α_b	$1.57336 \times 10^5 \text{ N m}^{-1} \text{ V}^{-1}$
c_{0b}	$1.6580 \times 10^3 \text{ N s m}^{-1} \text{ V}^{-1}$
k_{0b}	$1.384 \times 10^3 \text{ N s m}^{-1} \text{ V}^{-1}$
γ	2.85 m^{-1}
β	5.42 m^{-1}
V_{\max}	5 V

where η is the time constant associated with the first order filter and v is the command voltage applied to the current driver. The parameter values are given in Table 1. The time delay associated with the MR damper and the Wonder Box closed loop response together is less than 10 ms (Carrion and Spencer, 2007). The first natural frequency of the structure considered for the present study is 4.59 Hz. This translates to a substantially higher period than 10 ms. Moreover, this time delay is not significant in structural control applications as the earthquake time signal is updated every 10–20 ms interval. The Wonder Box contains a closed loop transfer function to compensate for changes in the electrical loads. A pulse width modulation with a frequency of 30 kHz (unfiltered) has been used for the current controller. The input control signal to the Wonder Box can be switched at a maximum rate of 1 kHz (Wonder Box, 2008). Eq. (3) can be used to account for the time-lag associated with the use of the Wonder Box.

Eqs. (1)–(3) show a nonlinear force ($u(t)$)–command voltage (v) relation. One can determine the force required to suppress the building vibration using various control algorithms, but it is very difficult to determine the voltage to be supplied to the damper to provide the required control force. This study describes the use of FLC to monitor the MR damper voltage based on the feedback from the structure. Acceleration and relative velocity at the damper location are taken as inputs ($UOD \in [-1, 1]$) to the FLC system and damper voltage ($[0, 1]$) is considered as an output. Five MFs are used for both the input variables, whereas seven MFs are used to map the output. An absolute function ('abs') is used to convert the FLC output (the output MFs ranges $[-1, 1]$) to MR damper voltage ($[0, 1]$). This is done to preserve the symmetry of the output MFs about zero.

3. Encoding fuzzy logic structure

Although fuzzy logic allows the creation of simple control algorithms, the tuning of the fuzzy controller for a particular application is a difficult task and one needs a more sophisticated procedure than that used for a conventional controller. This is due to the large number of parameters that are used to define the MFs and the inference mechanisms. Several methods have been developed for tuning fuzzy controllers. These involve adjustment of the MF (Arslan and Kaya, 2001) and/or scaling factors (Zhao and Collins, 2003) and dynamically changing the defuzzification procedure (Zheng, 1992). Previous effort towards optimization of FLC have employed strategies such as neural networks and neuro-fuzzy algorithms (Schurter and Roschke, 2001; Ali and Ramaswamy, 2007). Other researchers have turned to GA for development

of fuzzy controllers that manage active control schemes (Ali and Ramaswamy, 2007; Ahlawat and Ramaswamy, 2004). NSGA II optimized fuzzy rule base structure is reported by Shook et al. (2008) for a three storey laboratory scale building along with experimental results. A simple GA with local improvement mechanism applied to a smart base isolated system is reported by Kim and Roschke (2006). The main purpose of employing a GA is to determine appropriate fuzzy control rules as well to adjust parameters of the MFs. In the work (Kim and Roschke, 2006), the weighting factor associated with each rule is introduced into the chromosomes in order to let the GA weaken or strengthen the contribution of each rule. Therefore, the approach needs as many variables as there are rules to get an optimal rule base. The advantage of the approach reported in the present paper is that it takes only two variables to optimize the rule base geometry.

The FLC structure takes relative velocity and acceleration at the damper location as an input and provides damper voltage as an output ($v(t) \in [0, 1]$). The input variables are normalized over the UOD (universe of discourse) of $[-1, 1]$ using pre-scaling gains (selected using EA). The input variables range their respective UOD using five MFs (NL = negative large, NS = negative small, ZE = zero, PS = positive small and PL = positive large), whereas the output space is mapped using seven MFs (NE = negative and PO = positive are extra).

This paper studies two different FLC, whose parameters are optimized using μ -GA and PSO.

- FLC–FRB: GA optimizes the scaling gains, MFs shape and parameters keeping the rule base fixed. The rule base adopted is presented in Table 2.
- FLC–ORB: GA optimizes the scaling gains, MFs shape and parameters, as well as the rule base.

3.1. Encoding membership function

A generalized bell shaped (MATLAB, 2004) MF is used for all the inner MFs of the input–output variables, as it can assume any other MF shape. The extreme MFs for the input variables are kept unbounded in the respective positive (s-shaped) and negative (z-shaped) UOD (Jang et al., 2005). To minimize the computational cost associated with the optimization scheme, two variables are selected for optimization, namely, the MF width and the MF slope at 0.5 membership grade. The MF width is changed with a constraint that the overall span of all the MFs should range the UOD and each MF should maintain a 50% overlap with the neighbouring MFs. To enable evaluation of a nonuniform distribution of MFs, MF slope at 0.5 membership grade is encoded. This is achieved by multiplying the slope at 0.5 membership grade (of an uniformly distributed MFs) with a value between 0.5 and 2. The MF width is coded with 3 bits, which gives a precision of 0.0286 for a $\pm 10\%$ change in MF width. MF slope at 0.5 membership grade is coded with 4 bits in the binary string for μ -GA optimization. This gives a precision of 0.1 in the real value

Table 2
Rule base for FLC–FRB

Velocity	Acceleration				
	NL	NS	ZE	PS	PL
NL	NL	NE	NS	NS	ZE
NS	NE	NS	ZE	ZE	ZE
ZE	NS	ZE	ZE	ZE	PS
PS	ZE	ZE	ZE	PS	PO
PL	ZE	PS	PS	PO	PL

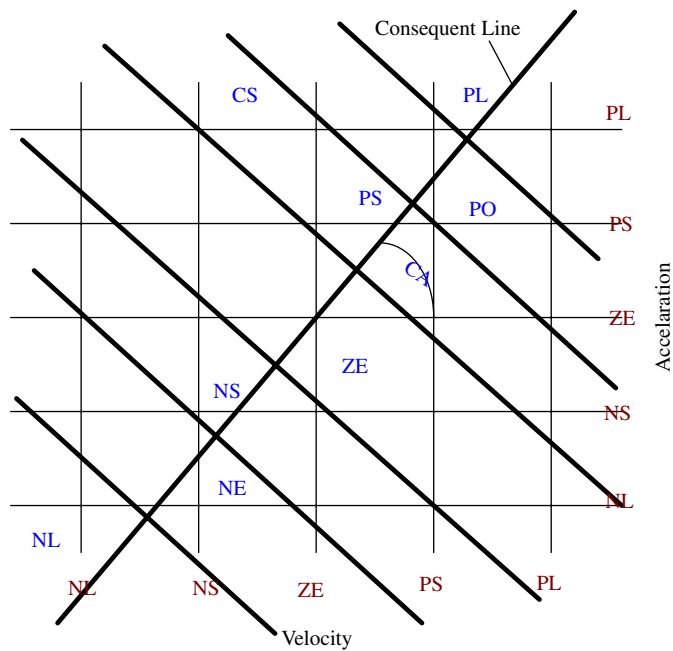


Fig. 1. Optimal rule base design.

for the multiplication factor of MF slope i.e., any value among $[0.5, 0.6, \dots, 2]$ can be used by the μ -GA.

3.2. Encoding rule base

To design an optimal rule base for the structural system we take advantage of the fact that control force input (and therefore the MR damper voltage) to the structure should increase when the structural responses increase i.e., the extreme input values (premise) result in extreme output values (consequent), mid-range input values result in mid-range output values and small/zero input values result in small/zero output values (Ahlawat and Ramaswamy, 2004; Ali and Ramaswamy, 2007). This rule base pattern is true for both the negative and positive portion of UOD.

A simple geometric approach is followed to modify the rule base (Byrne, 2003). For this a co-ordinate space is defined based on the premise MFs as shown in Fig. 1. The consequent space is then overlaid upon the 'premise coordinate system' and is in effect partitioned into seven nonoverlapping small regions, where each region represents a consequent fuzzy set (Fig. 1). The line diagonally crossing the co-ordinate space is defined as a 'consequent line'. This line has been made pivotal on premise zero-zero position (i.e. both inputs being zero) and it is free to rotate over the consequent space and therefore the rule base adapts according to the optimization scheme. A second variable ('consequent spacing') is chosen to define the width of region of output fuzzy sets over premise co-ordinate. The rule base is then extracted by determining the consequent region in which each premise combination point lies. Consequently, the present optimization is made possible by encoding only two variables (consequent-line angle, CA and consequent-region spacing, CS).

- Slope of the CA: It is used to create the output space partitions (angles between 0 and 180°). CA is coded with 5 bits in the binary string for binary GA optimization. This gives a precision of 0.1013 radian in real value.
- CS: As seen from Fig. 1 'CS' is a proportion of the fixed-distance between the premises (NS, NL, ZE, PS and PL) on the coordinate system and is used to define the distance between

consequent points along the consequent line. CS is coded with 4 bits to change the CS from half to twice its spacing as in FLC-FRB.

For consequent line angle of 45° and consequent region spacing of 1, we get a rule base analogous to the rule base that can be derived from the first mode vibration of the structure (Ahlawat and Ramaswamy, 2004). This rule base has been used later in the paper for simulation of the system with fixed rule base (see Table 2). The input scaling gains for relative velocity and acceleration are coded with five binary bits each.

4. Optimization of FLC

The optimization of the FLC variables proposed strategy is made possible using a μ -GA and a PSO technique. The advantage of these evolutionary optimization techniques is its ease in selection of a fitness functions. The fitness function can include variables that are not the state variables in the control system. In contrast, modern control theory that is based on the state space system can incorporate only state variables into the performance index.

4.1. Micro-GA

Micro-GA was proposed by Krishnakumar (1989) to improve the performance of GA with smaller population sizes. The μ -GA operates on a family, or population of designs similar to the simple GA but with a reduced population size. The basic idea is to use a smaller population GA and allow it to converge rapidly and invoke random population and start the search again (i.e., restart the GA) without changing the elitist chromosome. A μ -GA performs better in multi-modal optimization problems and is therefore suitable for the FLC optimization. To restart the GA search the current population has been aggressively mutated. In addition, Krishnakumar (1989) reported that μ -GA reaches the optimum in fewer function evaluations compared to the simple GA. This makes the application of μ -GA suitable for large scale problems and parallel processing (Pulido and Coello, 2003).

In this study, the μ -GA with the following specifications have been used.

- (1) Initial population search space is sub-divided into two complimentary subspaces. Half of the initial population is selected randomly and the other half is obtained by taking compliment of the initial half. In this manner any localization in initial population is minimized. It is reported (Krishnakumar, 1989) that even as few as a five member population can provide a global convergence. Here, we use an initial population size of seven members. Restart has been initiated at every 20th generation.
- (2) Gray encoding and decoding is used (Haupt and Haupt, 2004). Ordinary binary value representation in GA may sometimes be trapped in inefficient crossover (Haupt and Haupt, 2004) (i.e. offspring results in lesser fitness value than parents). Gray code avoids this problem by redefining the binary numbers such that the consecutive numbers have a Hamming distance of 1. Gray code is obtained by passing every consecutive binary numbers through a XOR operation.
- (3) A weighted multi-objective fitness function is adopted for the optimization of the FLC. The multi-objective fitness function consist of the sum individual fitness functions which are framed to minimize each of the states in L_2 norm sense and are described in Eq. (7).

- (4) Proportional fitness with stochastic universal sampling (SUS) is used (Haupt and Haupt, 2004). SUS is markedly different from roulette wheel selection technique. It is best described as a multi-pointer roulette wheel selection technique in which n (number of individuals in intermediate group) points are selected in the fitness line with the first one chosen randomly and others made equidistant from the previous one. Fitness values of the individuals within these points are selected. Individuals having higher fitness are given higher share of fitness line (as in roulette wheel) and therefore have a greater chance of selection. Since, SUS selects individuals in a single turn it is faster and more efficient than roulette wheel selection.
- (5) Two point cross-over with probability 0.4 is considered.
- (6) Mutation probability of 0.01 is taken for all iterations, and in the restart generation a 0.5 probability of mutation is considered.
- (7) The best member in each population in each generation is always carried to the next generation as done in an elitist approach.

Micro-GA optimizes eight variables (scaling gains for each of the inputs, MF width and MF slope for each of the inputs and one output) for FLC-FRB. This results in the binary coded chromosome of length 31 [2×5 (for scaling gains) + 3×3 (for MF width) + 3×4 (for MF slope)]. The optimization of FLC-ORB is carried out using a total of 40 bits in a single chromosome (as it contains the 5 bits representing the CA and 4 bits representing CS).

4.2. Particle swarm optimization

The PSO is a population based stochastic optimization technique developed by Kennedy and Eberhart (1995), inspired by social behaviour of bird flocking or fish schooling. It uses a number of particles that constitute a swarm. Each particle traverses the search space looking for the global optima. In a PSO system, particles fly around in a multidimensional search space. During flight, each particle adjusts its position according to its own experience, and the experience of neighbouring particles, making use of the best position encountered by itself and its neighbours. The swarm direction of a particle is defined by the set of particles neighboring the particle and its own past experience. PSO shares many similarities with other evolutionary computa-

tion techniques such as GA. The system is initialized with a population of random solutions. The population then search for the optima by updating in subsequent generations. However,

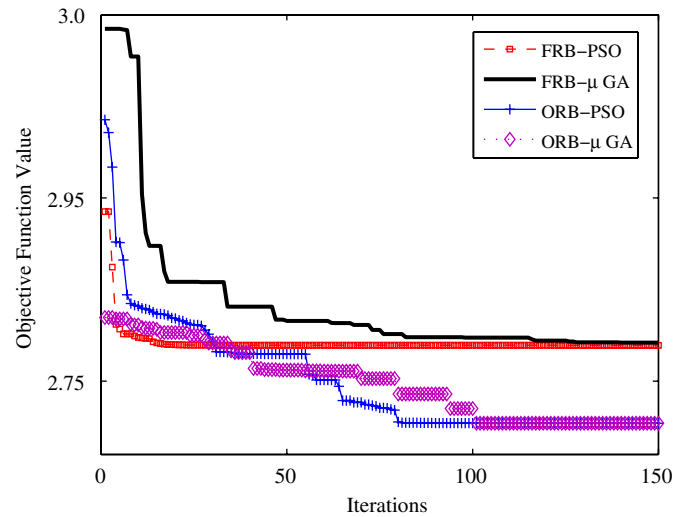


Fig. 3. Convergence of FLC optimization: MDOF case.

Table 3 Computational time required

Case	No. of function evaluation	Computational time	Optimal value
<i>SDOF optimization</i>			
FRB-μ-GA	7×100	9.9893×10^3	0.10613
ORB-μ-GA	7×150	28.527×10^3	0.08320
FRB-PSO	20×100	28.800×10^3	0.10612
ORB-PSO	20×150	113.99×10^3	0.08328
<i>MDOF optimization</i>			
FRB-μ-GA	7×150	56.508×10^3	2.55261
ORB-μ-GA	7×150	66.362×10^3	2.44510
FRB-PSO	20×150	163.059×10^3	2.54908
ORB-PSO	20×150	209.197×10^3	2.44246

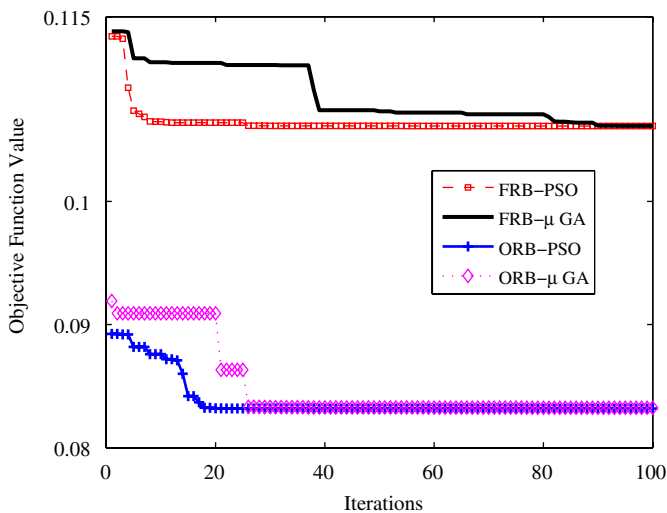


Fig. 2. Convergence of FLC optimization: SDOF case.

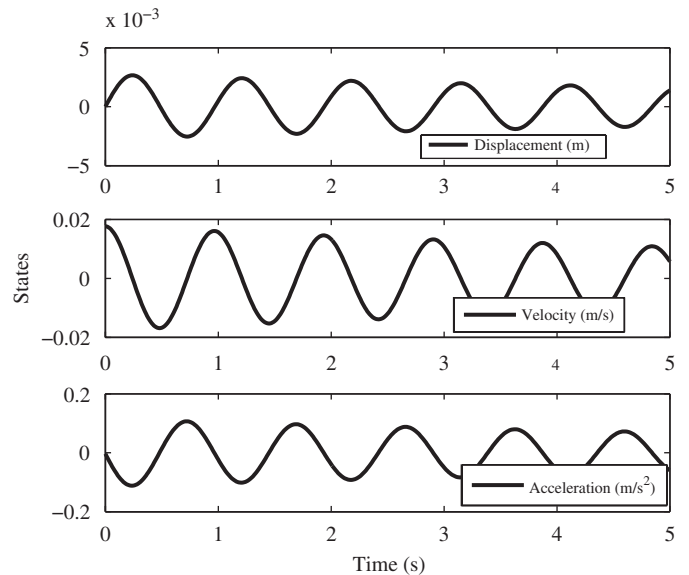


Fig. 4. Uncontrolled responses (SDOF system).

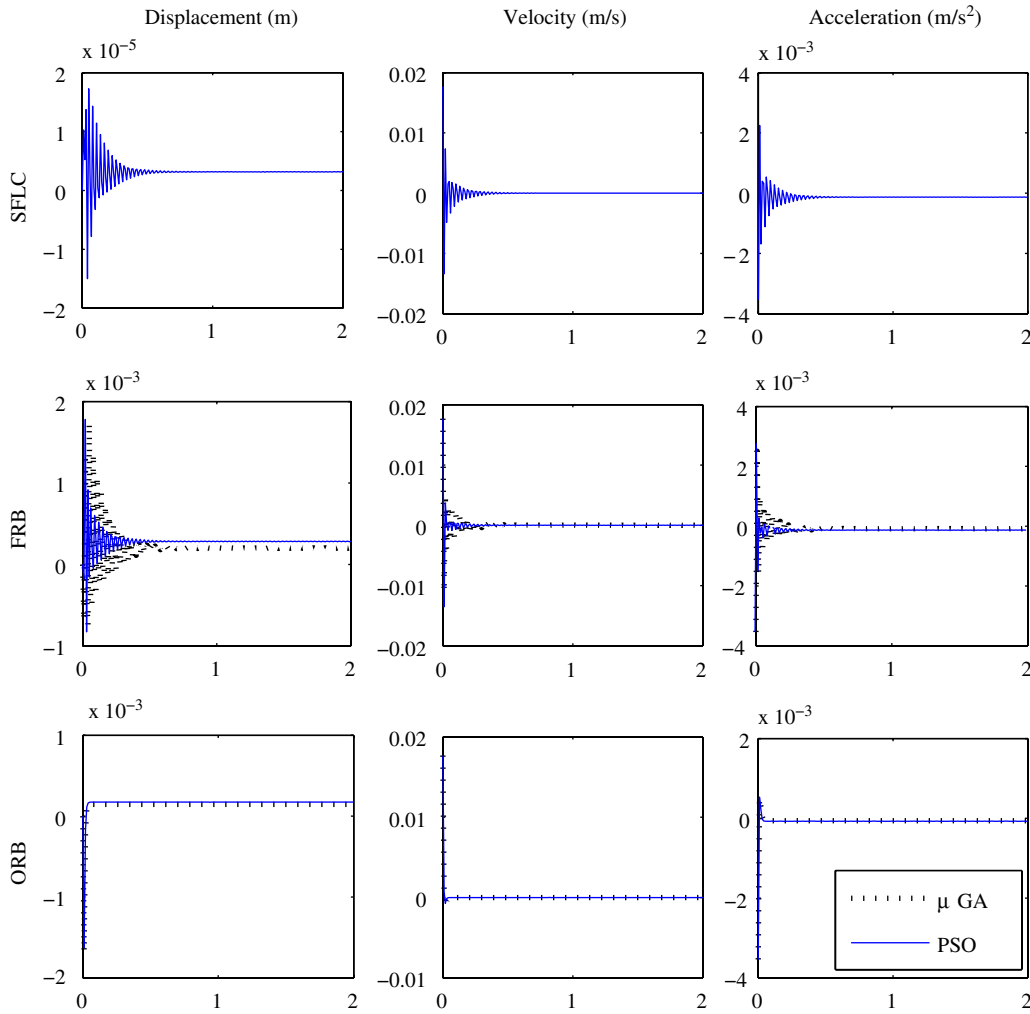


Fig. 5. Time history of FLC controlled SDOF system (displacement, velocity and acceleration).

unlike GA, PSO has no evolution operators such as crossover and mutation. Compared to GA, the advantages of PSO are that PSO is easy to implement and there are few parameters to adjust. PSO has been successfully applied in many areas, such as function optimization, artificial neural network training, fuzzy system control and other areas where GA can be applied. The working strategy of PSO is given next.

In the PSO scheme, Let x_p and v_p denote a particle position and its corresponding flight velocity in a search space, respectively. The best previous position of a particle is recorded and represented as pBest. The index of the best particle among all the particles in the group (taken as neighbour) is represented as gBest. Constriction function (C) is used to ensure convergence of PSO (Eberhart and Shi, 2000). The modified velocity and position of each particle can be calculated as shown in the following formulas:

$$\begin{aligned}
 v_{p_{g+1}} &= C[w \times v_{p_g} + \phi_1 c_1 \times (pBest - x_{p_g}) + \phi_2 c_2 \times (gBest - x_{p_g})] \\
 x_{p_{g+1}} &= x_{p_g} + v_{p_{g+1}}
 \end{aligned}
 \tag{4}$$

where g is the generation number, x_{p_g} is the current position of particle at generation g and v_{p_g} is the corresponding velocity of particle. $w = 1$ is the inertia weight factor, $\phi_1 = 2.05$ and $\phi_2 = 2.05$ are acceleration constants, c_1 and c_2 are uniform random values in the range $[0, 1]$, C is constriction factor which is a

function of ϕ_1 and ϕ_2 as given in the following equation:

$$\begin{aligned}
 C &= \frac{2}{\left| 2 - \phi - \sqrt{\phi^2 - 4\phi} \right|} \\
 \phi &= \phi_1 + \phi_2, \quad \phi > 4
 \end{aligned}
 \tag{5}$$

PSO is run to optimize the same cost functions and for same number of generations as μ -GA. Each swarm is considered to be consist of 20 members.

Figs. 2 and 3 show the convergence of μ -GA and PSO for both FRB and ORB FLCs. The fitness value and the computational time required are tabulated in Table 3. It is to be observed that both the optimization schemes converge to the nearly same fitness value but PSO converges faster in terms of number of generations (see Figs. 2 and 3). The computational time required by the PSO is much more than that of μ -GA, as PSO evaluates fitness function 20×150 number of times, whereas μ -GA evaluates it for only 7×150 . Therefore, where computational time is a constraint or each function evaluation takes large amount of time (as in case of large structures) μ -GA should be preferred to PSO. Alternatively, one has to use PSO with less number to generations (where a risk remains that PSO may converge to a non-global optima). Another interesting observation is that the ORB-FLC has lesser fitness function value than the corresponding FRB-FLC although both

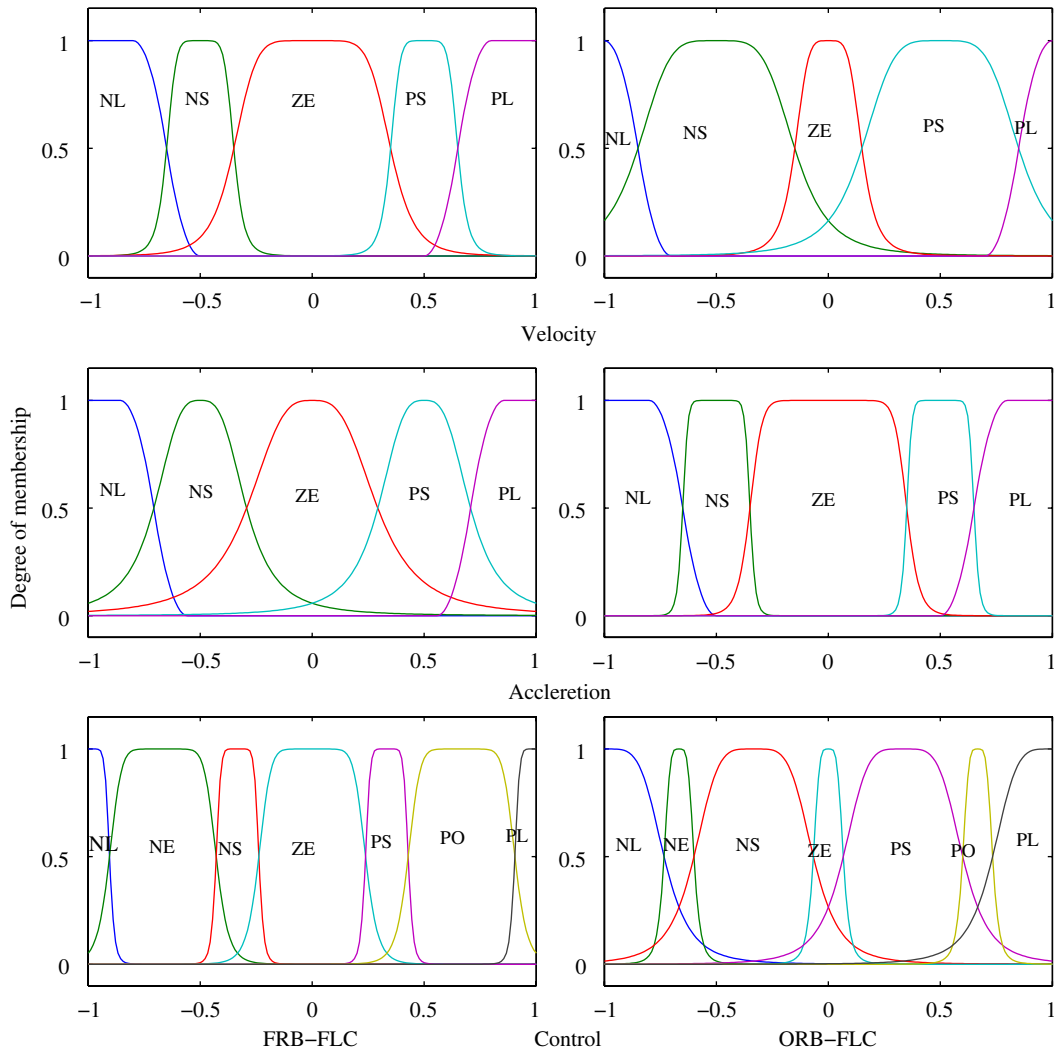


Fig. 6. μ -GA optimized input/output MFs (MDOF system).

used the same fitness function. This represents a better control of the structure using optimal rule base strategy.

5. Numerical simulation and results

Numerical simulations are carried out for three different cases. First an SDOF system is taken and its vibration (under impulsive load) is minimized using optimized FLCs. All the four cases namely (i) FRB-PSO: fixed rule base FLC optimized using PSO, (ii) FRB- μ -GA: fixed rule base FLC optimized using μ -GA, (iii) ORB-PSO: optimal rule base FLC optimized using PSO, (iv) ORB- μ -GA: optimal rule base FLC optimized using μ -GA, are applied and a comparative analysis is performed. Next a three storey building example (subjected to impulsive load) is taken for the comparative analysis of the above four techniques. Finally, based on the μ -GA optimized FLCs (both FRB and ORB) obtained in the second case, performance evaluation of the same three storey building under a set of seismic records is performed and reported.

5.1. SDOF system

An SDOF model has been taken for the *impulse response analysis* of the proposed fuzzy logic systems. A base isolated building performs as an SDOF system. Therefore, it can be thought

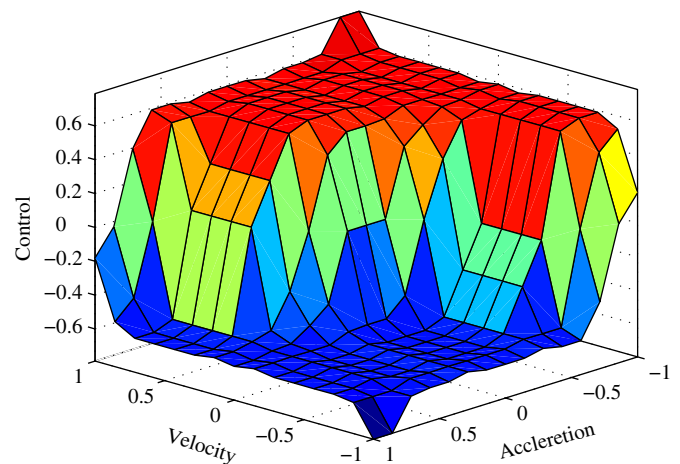


Fig. 7. μ -GA optimized fuzzy rule base (MDOF system).

of as a base isolated building structure. The equation of motion of the SDOF system is given as

$$\begin{aligned}
 m\ddot{x} + c\dot{x} + kx &= u(t) \\
 x(0) = 0, \quad \dot{x} &= \frac{1}{m}
 \end{aligned}
 \tag{6}$$

where $m = 56.52 \text{ kg}$, $c = 11.30 \text{ N s m}^{-1}$, $k = 2.375 \times 10^3 \text{ N m}^{-1}$ are system mass, damping and stiffness parameters, respectively. $u(t)$ is the restoring force provided by the MR damper. (\cdot) represents derivative with respect to time (t). The system is driven by giving an initial velocity of $\dot{x}(0) = 1/m$ to simulate the system response to an impulsive force. The objective is to bring the system responses to zero. The FLC has been trained using μ -GA and PSO to minimize L_2 norm of displacement, velocity and acceleration responses of the system. The fitness function is the main criterion that is used to evaluate each chromosome. It provides an important connection between the EA and the physical system that is being modeled. A controller should minimize the structural displacement without increasing the acceleration. Large displacement is catastrophic to the structure where as acceleration effects the occupant comfort and the contents inside. Additionally, MR damper depends on the structural velocity and therefore minimization of structural velocity is also taken into consideration in fitness function.

There are several methods that can combine multiple objective functions to make a single fitness function in a multi-objective optimization problem. One of these methods, a weighted sum approach, is employed in this study as shown in Eq. (7). As these three objectives impose conflicting requirements, the relative importance of these goals must be selected by the designer. The displacement, velocity and acceleration are normalized with respect to their corresponding uncontrolled L_2 norm values (represented with subscript unc).

$$\Phi_1(t) = w_1 \times \frac{\|x(t)\|}{\|x_{unc}(t)\|} + w_2 \times \frac{\|\dot{x}(t)\|}{\|\dot{x}_{unc}(t)\|} + w_3 \times \frac{\|\ddot{x}(t)\|}{\|\ddot{x}_{unc}(t)\|} \quad (7)$$

where $\|\cdot\|$ denotes the L_2 norm of the state variables. Equal weights ($w_i = 1, i = 1, 2, 3$) are taken for all the objective functions. The simulation has been run for 5 s as the controlled responses has seen to achieve the goal well before 5 s.

Fig. 2 shows the convergence of the PSO and μ -GA for fixed rule base and optimal rule base case. It is to noted that the fitness function for FLC–FRB has higher objective value than that of the FLC–ORB, which shows that the optimal rule base FLC provides a better control of the SDOF system. PSO is seen to converge faster than μ -GA, whereas μ -GA takes lesser time to converge as the number of function evaluation required in μ -GA is far less than in PSO. This advantage of μ -GA makes it more viable for on-line applications. The number of function evaluation and the time taken on a P4 desktop PC with 2.8 GHz processor speed is tabulated in Table 3.

Fig. 4 shows the time history of the uncontrolled system responses for 5 s. The system responses continues even after 5 s of vibration as the damping is very low. The controlled responses are shown in Fig 5. The controlled system responses are shown for 2 s for clarity in the figure. Fig. 5 contains results obtained from FLC manually configured (SFLC), FLC with optimal MF and scaling gains (FRB) and FLC with optimal MF, scaling gains and rule base (ORB). The results obtained through μ -GA optimization (dashed line) and PSO (solid line) are shown together for better comparison. It is evident from Fig. 5 FLC–FRB performs better than SFLC but FLC–ORB performs far better than FLC–FRB and SFLC.

5.2. MDOF system

The equation of motion of the three storey shear building model, taken for seismic mitigation analysis is given in the following equation:

$$M\ddot{X} + C\dot{X} + KX = Af(t) + M\Gamma\ddot{x}_g \quad (8)$$

where $X = \{x_1, x_2, x_3\}^T$ is the vector of floor displacements relative to the ground, subscript denotes storey number. \ddot{x}_g is the seismic ground acceleration. M and K are mass and stiffness matrices, respectively,

$$M = \begin{bmatrix} 56.52 & 0 & 0 \\ 0 & 56.52 & 0 \\ 0 & 0 & 56.52 \end{bmatrix} \text{ kg},$$

$$K = \begin{bmatrix} 4.75 & -2.375 & 0 \\ -2.375 & 4.75 & -2.375 \\ 0 & -2.375 & 2.375 \end{bmatrix} \times 10^5 \text{ N m}^{-1} \quad (9)$$

C is the Rayleigh damping matrix and is constructed using 0.5% modal damping in all modes. The Rayleigh parameter (α_d, β_d) are determined based on the first and third eigen frequencies (ω_1, ω_3) of the system (Chopra, 2005). Eq. (10) shows the construction of the damping matrix.

$$C = \alpha_d M + \beta_d K$$

$$\alpha_d = 2 \frac{\zeta \omega_1 \omega_3}{\omega_1 + \omega_3}, \quad \beta_d = 2 \frac{\zeta}{\omega_1 + \omega_3} \quad (10)$$

$A = [1 \ 0 \ 0]^T$ is the co-efficient vector determining the position of the damper (in this case damper is located at the first floor of the building), $\Gamma = [1 \ 1 \ 1]^T$ is the seismic influence vector.

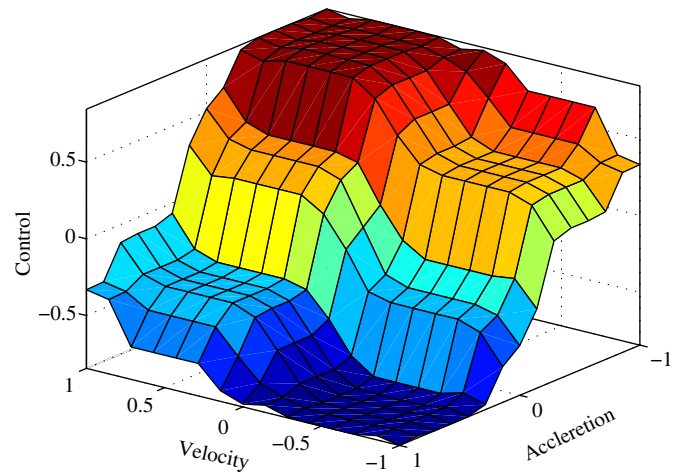


Fig. 8. PSO optimized fuzzy rule base (MDOF system).

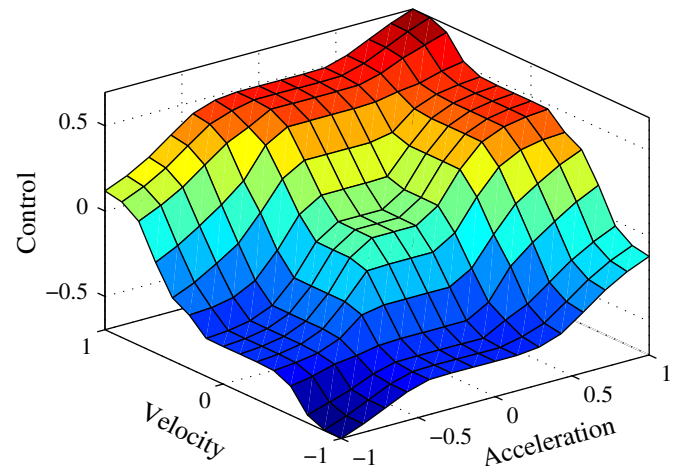


Fig. 9. GA optimized fuzzy rule base for three input MFs and five output MFs.

The FLC is optimized for an initial displacement of 0.1 m and then the motion is allowed to decay under free vibration condition. The idea is to optimize the FLC to minimize the structural motion quickly when excited by a sudden base displacement which is a character of near source seismic motions. Optimization is performed using both μ -GA and PSO and the objective function used is similar to that of the SDOF case, the only

difference is that the normalized response L_2 norms are summed over all the floors.

$$\Phi_2 = \sum_{\text{floors}} \left(\frac{\|x(t)\|}{\|x_{\text{unc}}(t)\|} + \frac{\|\dot{x}(t)\|}{\|\dot{x}_{\text{unc}}(t)\|} + \frac{\|\ddot{x}(t)\|}{\|\ddot{x}_{\text{unc}}(t)\|} \right) \quad (11)$$

The convergence curves of the optimization schemes are shown in Fig. 3. It is evident from Fig. 3 that optimal rule base FLC performs better than fixed rule base FLC. Micro-GA and PSO provide the same optimal cost (see Table 3). Fig. 6 shows all the input–output MFs for both FLC–FRB and FLC–ORB obtained using μ -GA. It is to be noted that the MFs has 50% overlap with each other and they range the domain of UOD, i.e. $[-1, 1]$, which are taken as constraints while generating MFs genetically. The μ -GA optimized and PSO optimized input–output relation surface plots for FLC–ORB are shown in Figs. 7 and 8, respectively. Both the optimization schemes provide similar nature of rule surface.

To observe the effect of using fewer MFs on the input and output MFs, we have considered simulation of ORB–FLC with three input MFs (namely, NL, ZE and PL) and five output MFs (namely, NL, NS, ZE, PS and PL) for the MDOF system. The time taken for the optimization with μ -GA is 42.33×10^3 s. Fig. 9 shows the optimal rule obtained in the simulation. It is observed that the optimal rule surface is similar to that of obtained in ORB–FLC with five input MFs and seven output MFs. Fig. 10 shows the comparative plots for ORB–FLC with three input–five output MFs and ORB–FLC with five input–seven output MFs. First floor displacement and acceleration time history normalized with

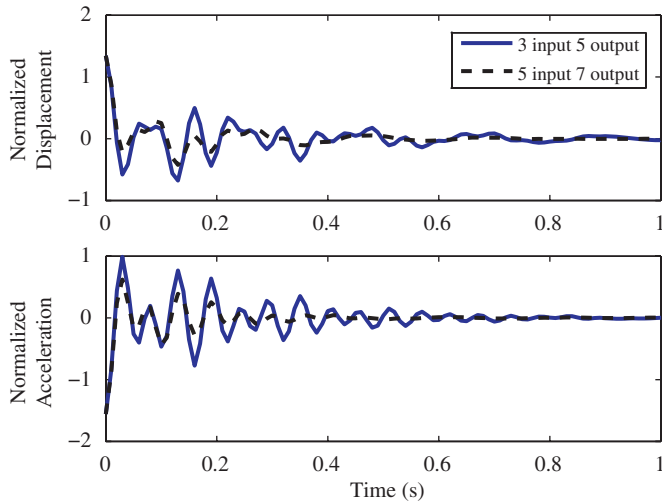


Fig. 10. Time history of normalized responses (first floor).

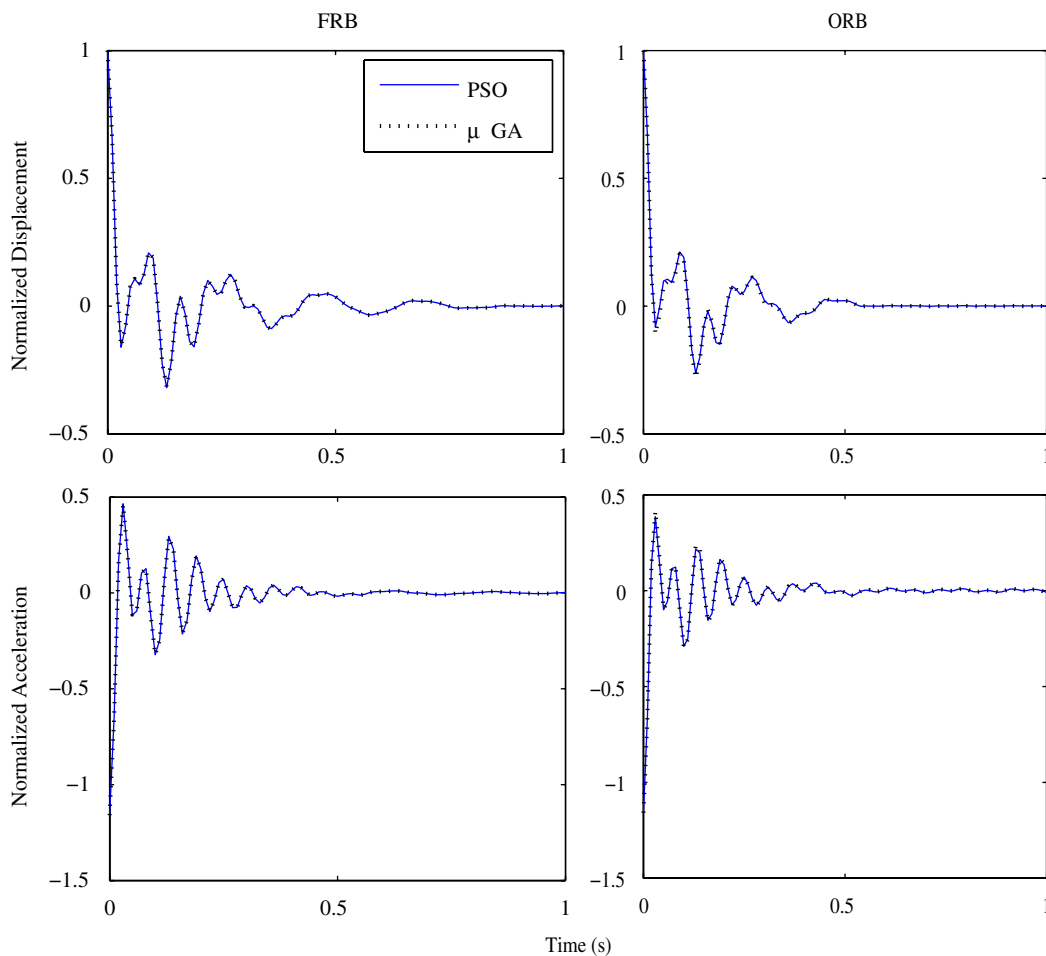


Fig. 11. Time history of normalized responses (first floor).

respective to the corresponding peak uncontrolled values are shown in Fig. 10. It is evident from Fig. 10 that the ORB-FLC with five input–seven output MFs provide slightly better performance than that with fewer MFs. Thus subsequent analysis has been reported for five input and seven output MFs.

MDOF structural displacement and acceleration responses obtained from first and third floor of the building are shown in Figs. 11 and 12. For clarity in the figures the responses are shown for a duration of 1 s. Figs. 11 and 12 contain responses obtained using PSO and μ -GA optimization for both FLC-FRB and FLC-ORB. The responses are normalized with respect to their corresponding uncontrolled cases. It is to be noted that the results obtained through PSO and μ -GA match. The corresponding controlling force provided by the damper and the voltage input are shown in Fig. 13.

5.3. Seismic vibration mitigation

A set of seismic records consisting of Chichi, Elcentro-1940 and Northridge earthquake data are considered for the performance analysis of the three storey building using optimal FLC. As shown in the preceding example that the results of FLC-FRB and FLC-ORB optimized using μ -GA match with the corresponding results obtained using PSO, therefore, the optimal FLCs obtained using μ -GA are considered for the seismic vibration mitigation of the building.

A set of performance indices is defined to determine the efficiency of the control techniques used for the study.

$$J_1 = \frac{\max_t |x_c(t)|}{\max_t |x_{unc}(t)|}, \quad J_2 = \frac{\max_t |\dot{x}_c(t)|}{\max_t |\dot{x}_{unc}(t)|}, \quad J_3 = \frac{\max_t |\ddot{x}_c(t)|}{\max_t |\ddot{x}_{unc}(t)|}$$

$$J_4 = \frac{\|x_c(t)\|}{\|x_{unc}(t)\|}, \quad J_5 = \frac{\|\dot{x}_c(t)\|}{\|\dot{x}_{unc}(t)\|}, \quad J_6 = \frac{\|\ddot{x}_c(t)\|}{\|\ddot{x}_{unc}(t)\|} \tag{12}$$

where the subscript ‘c’ denotes the controlled responses and the subscript ‘unc’ represents the uncontrolled motion. \max_t represents maximum value over time (t), $|x|$ denotes the absolute value of x and $\|x\|$ denotes the L_2 norm of x.

The performance of the system according to Eq. (12) for all three seismic records is tabulated in Table 4 for both FLC-FRB and FLC-ORB. Comparing the results presented in Table 4, one can see that FLC-ORB is better than FLC-FRB in controlling all responses of the structure. Normed first floor velocity is the only case where FLC-FRB has shown better performance than that of FLC-ORB, the reason is that FLC-ORB adds more force to the system to mitigate its vibration which increases the velocity response at the damper location.

Fig. 14 shows the uncontrolled and controlled floor displacements of the building under Chichi, Elcentro and Northridge earthquake ground motions. It is seen that the FRB-ORB does not only reduce the peak floor responses but also minimizes the floor drifts. Fig. 15 shows the control force and the voltage required for FLC-FRB and FLC-ORB for Chichi earthquake. One should observe from Fig. 15 that the voltage supplied to the MR damper takes any

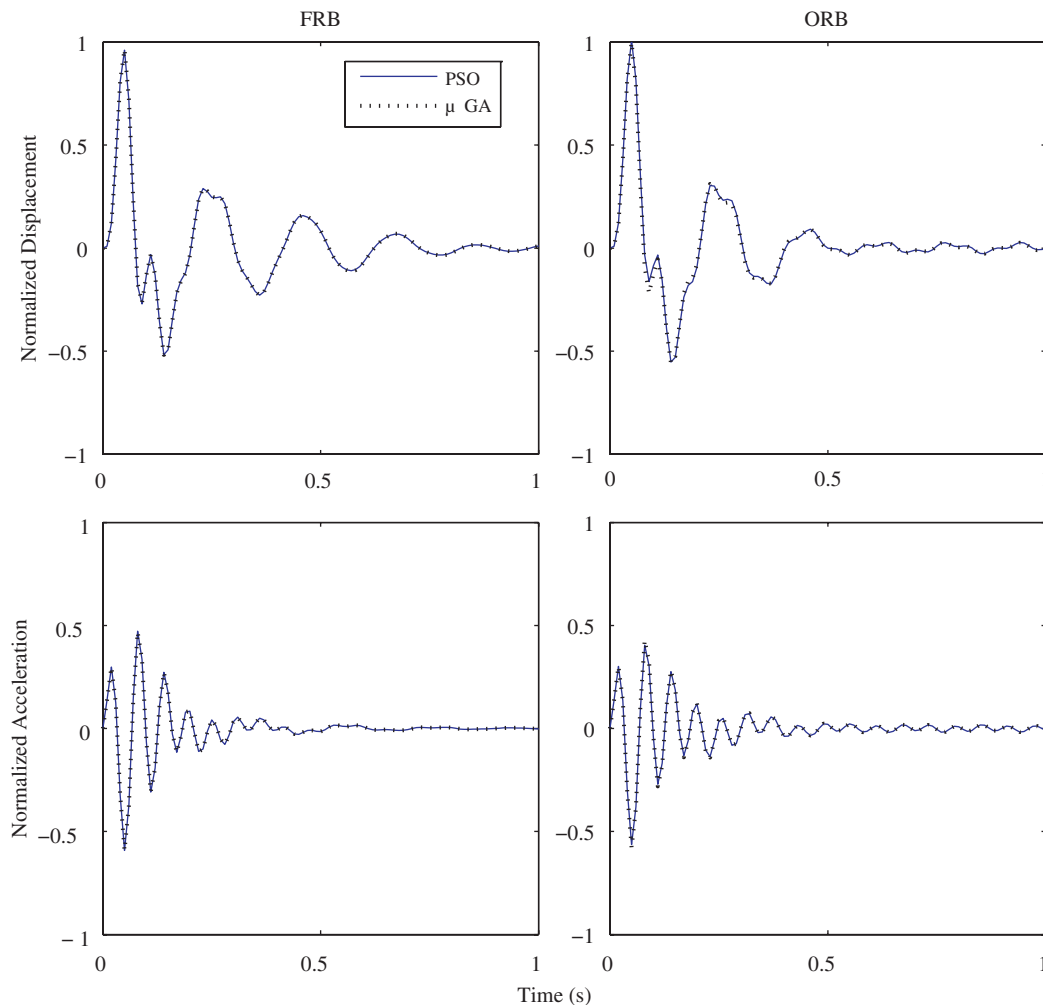


Fig. 12. Time history of normalized responses (third floor).

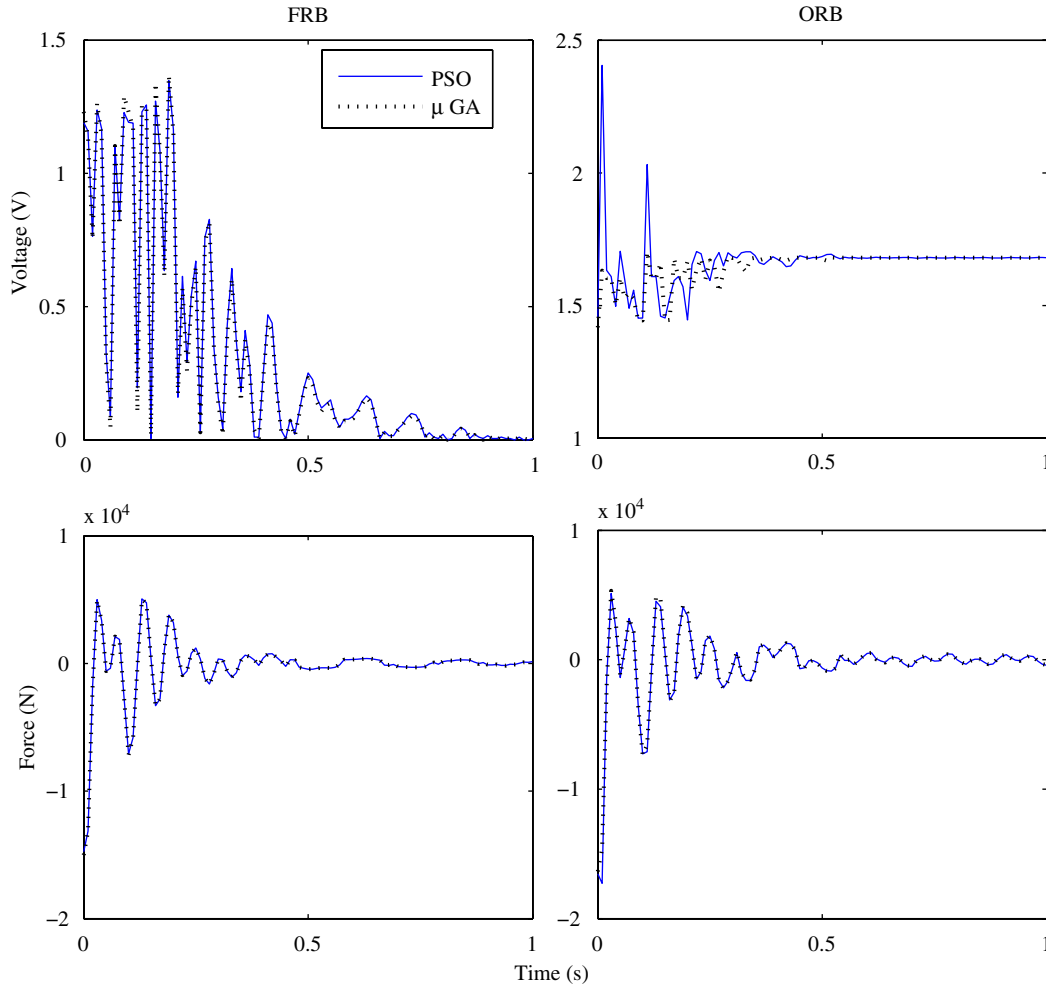


Fig. 13. Input voltage and control force (MDOF system).

Table 4

Performance indices: FF = first floor, SF = second floor and TF = third floor

PI	Floor	Chichi		Elcentro		Northridge	
		ORB	FRB	ORB	FRB	ORB	FRB
J_1	FF	0.2372	0.264	0.1311	0.187	0.235	0.2869
	SF	0.3351	0.4304	0.2372	0.3451	0.3268	0.3753
	TF	0.3885	0.5086	0.2777	0.4005	0.3621	0.4149
J_2	FF	0.219	0.2093	0.1284	0.2065	0.2184	0.2516
	SF	0.4682	0.5193	0.3005	0.3972	0.3108	0.3139
	TF	0.5338	0.6031	0.3443	0.5022	0.358	0.3723
J_3	FF	1.4536	2.0051	1.3987	2.2985	1.3014	1.4814
	SF	0.4676	0.6238	0.4658	0.6239	0.5229	0.609
	TF	0.7517	0.8508	0.467	0.7125	0.4594	0.5693
J_4	FF	0.1671	0.1916	0.0863	0.1183	0.2211	0.2481
	SF	0.2581	0.3173	0.2176	0.2902	0.3284	0.3681
	TF	0.2941	0.3829	0.2633	0.3609	0.3744	0.4337
J_5	FF	0.0927	0.06	0.0682	0.0439	0.1493	0.1205
	SF	0.2477	0.3803	0.2676	0.3765	0.353	0.4286
	TF	0.3011	0.4808	0.3293	0.4762	0.4215	0.5294
J_6	FF	1.3821	2.2322	1.4469	2.2368	1.4216	1.9704
	SF	0.4507	0.5881	0.4065	0.5476	0.5517	0.6589
	TF	0.4656	0.682	0.4595	0.6606	0.5753	0.7214

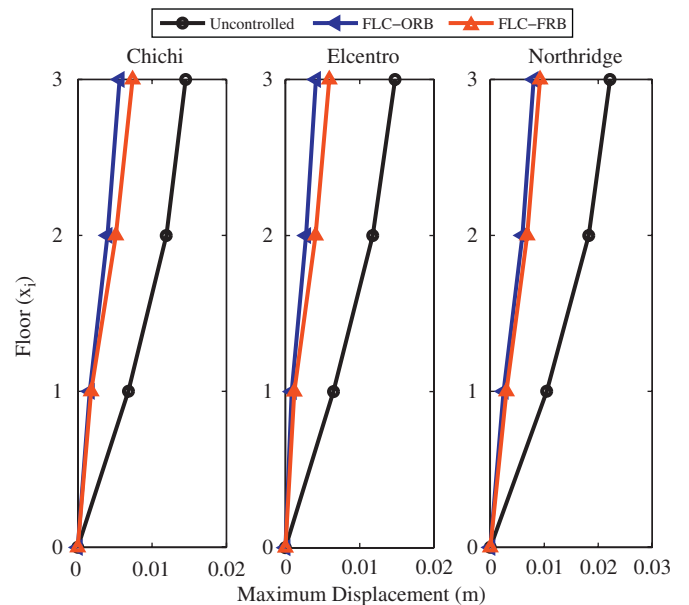


Fig. 14. Maximum floor response of three storey building (ChiChi, Elcentro and Northridge).

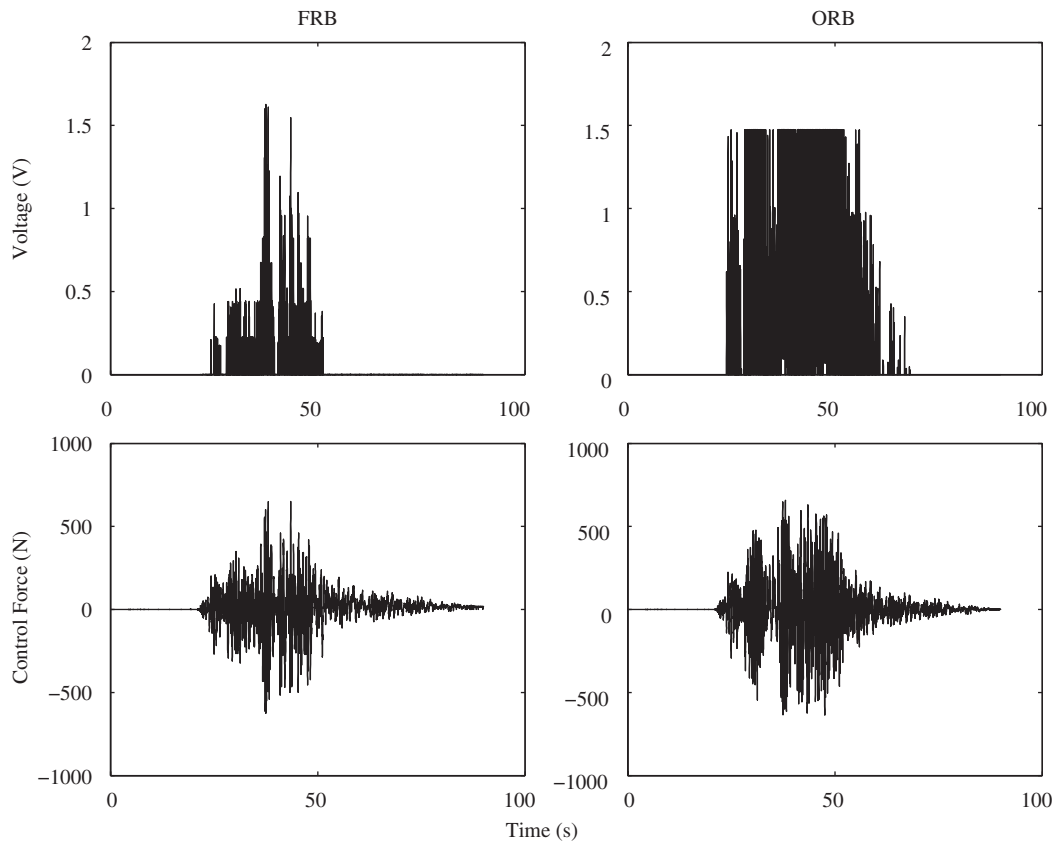


Fig. 15. Input voltage and control force time history (Chichi earthquake).

voltage value within its range and seldom reaches its maximum voltage value (5V).

6. Conclusion

This paper presents and compares several optimal FLCs used to monitor voltage input to the nonlinear hysteretic MR damper systems attached to a three storey building. Examples of SDOF and MDOF system under various conditions show that FLC monitored MR damper voltage effectively minimizes structural vibration. Furthermore, FLC driven MR damper voltage monitoring provides a gradual and smooth change of voltage and thereby increases the system stability. The paper also describes an easy and computationally less intensive technique to modify the rule base, which uses a minimum number of optimization variables. It is shown using an example of a three storey shear building model under base excitation and seismic ground motion that the FLC with optimal rule base modified using the proposed technique performs better than the conventional FLC with predefined rule base. The optimization of FLC is carried out using μ -GA and PSO with a constriction function. Results show that PSO converges faster in terms of number of generations than μ -GA but takes larger time and more function evaluation than that of μ -GA. Relative merits and demerits of the optimization schemes are discussed. Finally, the study evaluates the performance of the fuzzy controller trained off-line on a three storey building model under a set of earthquake records. It is seen that the present approach provides better vibration control for structures under earthquake excitations.

Acknowledgements

The authors are thankful to the unknown reviewers, whose suggestions have significantly enhanced the quality of the paper.

References

- Ahlawat, A.S., Ramaswamy, A., 2004. Multiobjective optimal fuzzy logic controller driven active and hybrid control systems for seismically excited nonlinear buildings. *Journal of Engineering Mechanics* 130 (4), 416–423.
- Ali, Sk.F., Ramaswamy, A., 2006. FLC based semi-active control of buildings using magneto-rheological dampers. In: Maity, D., Dwivedy, S.K. (Eds.), *Proceedings of the 2nd International Congress on Computational Mechanics and Simulation*. Indian Institute of Technology, Guwahati, India.
- Ali, Sk.F., Ramaswamy, A., 2007. Developments in structural optimization and applications to intelligent structural vibration control. In: Lagaros, N., Tsompanakis, Y. (Eds.), *Intelligent Computational Paradigms in Earthquake Engineering*. Idea Group Publishing, New York, pp. 125–247.
- Ali, Sk.F., Ramaswamy, A., 2008a. GA optimized FLC driven semi-active control for phase II smart nonlinear base isolated benchmark building. *Structural Control & Health Monitoring* 15 (5), 797–820.
- Ali, Sk.F., Ramaswamy, A., 2008b. Testing and modeling of MR damper and its application to SDOF systems using integral backstepping technique. *Journal of Dynamical Systems Measurement and Control*, ASME, submitted for publishing, accepted, in press.
- Arslan, A., Kaya, M., 2001. Determination of fuzzy logic membership functions using genetic algorithms. *Fuzzy Sets and Systems* 118, 297–306.
- Byrne, J.P., 2003. GA-optimization of a fuzzy logic controller. Masters Thesis, School of Electronic Engineering, Dublin City University.
- Carrion, J.E., Spencer Jr., B.F. 2007. Model-based strategies for real-time hybrid testing. NSEL Report Series, Report no. NSEL-006. Department of Civil and Environmental Engineering, University of Illinois at Urbana-Champaign.
- Chopra, A.K., 2005. *Dynamics of Structures: Theory and Application to Earthquake Engineering*. Pearson Education, New Delhi, India.
- Dounis, A.I., Tiropanisy, P., Syrcos, G.P., Tseles, D., 2007. Evolutionary fuzzy logic control of base-isolated structures in response to earthquake activity. *Journal of Structural Control and Health Monitoring* 14, 62–82.
- Dyke, S.J., Spencer Jr., B.F., Sain, M.K., Carlson, J.D., 1996. Modeling and control of magnetorheological dampers for seismic response reduction. *Smart Materials & Structures* 5, 565–575.
- Eberhart, R.C., Shi, Y., 2000. Comparing inertia weights and constriction factors in particle swarm optimization. In: *Proceedings of the Congress on Evolutionary Computing*, CA, USA, pp. 84–88.
- Feng, Q., Shinozuka, M., 1990. Use of a variable damper for hybrid control of bridge response under earthquake. In: *Proceedings of the U.S. National Workshop on Structure and Control Research*. University of Southern California, Los Angeles, pp. 107–112.

- Haupt, R.L., Haupt, S.E., 2004. *Practical Genetic Algorithm*, second ed. Wiley, New Jersey.
- Ikhouanea, F., Manosab, V., Rodellara, J., 2005. Adaptive control of a hysteretic structural system. *Automatica* 41, 225–231.
- Jang, J.S.R., Sun, C.T., Mizutani, E., 2005. *Neuro Fuzzy and Soft Computing*. Pearson Education, New Delhi, India.
- Jansen, L.M., Dyke, S.J., 2000. Semiactive control strategies for MR dampers: comparative study. *Journal of Engineering Mechanics, ASCE* 126 (8), 795–803.
- Karnopp, D.C., Crosby, M.J., Harwood, R.A., 1974. Vibration control using semi-active force generators. *Journal of Engineering for Industry* 96 (2), 619–626.
- Kennedy, J., Eberhart, R., 1995. Particle swarm optimization. In: *Proceedings of IEEE International Conference on Neural Networks*, Perth, Australia, pp. 1942–1948.
- Kennedy, J., Eberhart, R.C., 1999. The particle swarm: social adaptation in informal-processing systems. In: Corne, D., Dorigo, M., Glover, F. (Eds.), *New Ideas in Optimization*. McGraw-Hill, UK, pp. 379–387.
- Kim, H.-S., Roschke, P.N., 2006. Design of fuzzy logic controller for smart base isolation system using genetic algorithm. *Engineering Structures* 28, 84–96.
- Krishnakumar, K., 1989. Microgenetic algorithms for stationary and nonstationary function optimization. In: Rodriguez, G. (Ed.), *Proceedings of the SPIE Intelligent Control and Adaptive Systems*, vol. 1196, pp. 289–296.
- Leitmann, G., 1994. Semiactive control for vibration attenuation. *Journal of Intelligent Material Systems and Structures* 5, 841–846.
- MATLAB, 2004. *The Software for Numerical Computing*, version 7.0.1 (R14). The MathWorks.
- Pulido, G.T., Coello Coello, C.A., 2003. The micro genetic algorithm 2: towards online adaptation in evolutionary multiobjective optimization. In: Fonseca, C.M., Fleming, P.J., Zitzler, E., Deb, K., Thiele, L. (Eds.), *Evolutionary Multi-criterion Optimization*. Springer, Berlin, pp. 252–266.
- Schurter, K.C., Roschke, P.N., 2001. Neuro-fuzzy control of structures using acceleration feedback. *Smart Materials & Structures* 10, 770–779.
- Shook, D.A., Roschke, P.N., Lin, P.-Y., Loh, C.-H., 2008. GA-optimized fuzzy logic control of a large-scale building for seismic loads. *Engineering Structures* 30, 436–449.
- Soong, T.T., Spencer, B.F., 2002. Supplemental energy dissipation: state of the art and state of the practice. *Engineering Structures* 24, 243–259.
- Spencer, B.F., Dyke Jr., S.J., Sain, M.K., Carlson, J.D., 1997. Phenomenological model for magnetorheological dampers. *Journal of Engineering Mechanics, ASCE* 123 (3), 230–238.
- Wonder Box, 2008. LORD Device Controller Kit. (<http://www.lordfulfillment.com/upload/UI7000.pdf>), (downloaded: July 2008).
- Yang, G., Spencer, B.F., Carlson Jr., J.D., Sain, M.K., 2002. Large-scale MR fluid dampers: modeling and dynamic performance considerations. *Engineering Structures* 24, 309–323.
- Zhao, Y., Collins Jr., E.G., 2003. Fuzzy parallel parking control of autonomous ground vehicles in tight spaces. In: *IEEE International Symposium on Intelligent Control*, Houston, TX, pp. 811–816.
- Zheng, L., 1992. A practical guide to tune of proportional and integral (PI) like fuzzy controllers. In: *First IEEE International Conference on Fuzzy Systems*, San Diego, pp. 633–640.